Numerical study of a buried periodic device for vibration protection

Luís Godinho
ISISE, Dep. Civil Engineering, University of Coimbra, Portugal.

Carlos Albino
ISISE, Dep. Civil Engineering, University of Coimbra, Portugal.

Pedro Alves-Costa
Construct-FEUP, University of Porto, Portugal.

Paulo Amado-Mendes
ISISE, Dep. Civil Engineering, University of Coimbra, Portugal.

Alexandre Pinto
Construct-FEUP, University of Porto, Portugal.

Delfim Soares Jr.
Dep. Structural Engineering, Federal University of Juiz de Fora, Brazil.

Summary
Well-known classical strategies to mitigate vibrations induced by vehicles include buried trenches and inertia blocks. Besides these strategies, innovative methods are being devised by researchers using novel physical concepts. Periodic structures and metamaterials are one such concept, which seem to be a very promising for real engineering applications. These devices interfere with wave propagation in a controlled and tuned manner, and can be used for specific frequency bands. Some of these concepts are well-developed for acoustic protection (noise barriers), as is the case of "sonic" or "phononic" crystals, but the protection of vibrations by such structures is still in an earlier development stage. The present paper presents a preliminary study on the concept of using a periodic buried structure, made of repeated solid elements, disposed with a geometrical arrangement that allows maximization of the shielding effect in the dominant vibration frequencies. The 3D finite element model, formulated using tetrahedral elements, is used to perform a set of numerical simulations, assessing the effectiveness of the proposed shielding device. The model simulates a set of elastic inclusions, buried in a homogeneous host soil, under the incident of a propagating wave generated by a line source. In order to improve computational efficiency, a time-marching algorithm is used, and the time domain signals are then transformed to the frequency domain by means of a FFT, allowing calculation of insertion loss results at receivers placed behind the shielding device. The presented results reveal a good efficiency of these devices, and evidence the existence of a band gap where large attenuation occurs. Comparison with results obtained for a standard buried wall also allowed to observe that the use of the proposed strategy can lead to better attenuation results.

PACS no. 43.35.Cg, 43.35.Zc, 43.40.Le

1. Introduction and motivation

Mitigation of vibrations that can affect sensible constructions has been under discussion since the middle of last century when high-speed trains, with speeds above 200 km/h, emerged as regular intercity transport [1]. Since then, people's health and comfort have become a top priority. In this sense, the concern with the vibrations extends to the other transport systems, existing already several strategies of mitigation like the well-known trenches or buried walls. Nowadays, along with these classic strategies, new and innovative methodologies are being developed, assuming their greater efficiency, using new physical concepts. These concepts are widely developed in the case of

acoustic barriers and are at an early stage with respect to vibration mitigation. In the case of vibration mitigation, this concept is defined by periodic buried structures (see Figure 1), disposed in a geometrical arrangement, resulting in an efficient barrier to the dominant vibration frequencies.

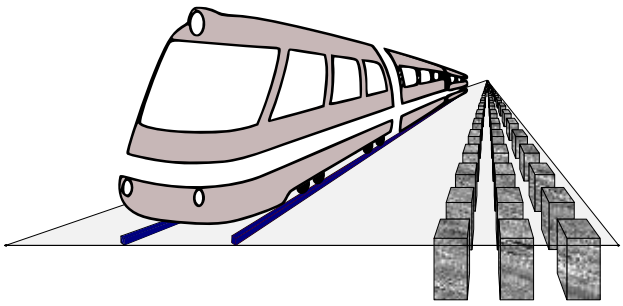

Figure 1– New mitigation devices (inclusions)

The present paper follows previous works by the authors in which numerical simulations are used to better understand the propagation of vibrations in the presence of periodic buried structures [2,3,4,5]. Here, to help simulate the effect of the inclusion of those periodic structures, an innovative time-marching algorithm supported by the 3D finite element method was used [6].

2. Waves propagation

In a solid material excited by mechanical impulses, three important types of waves are generated. The compression waves (P) are those with the highest propagation velocity, defined by equation 1 (E, ν and ρ being the Young modulus, Poisson ratio and density). Those are longitudinal waves causing displacements in the medium, parallel to the direction of the wave. The shear waves (S) are transverse waves causing displacements in the medium, and they are perpendicular to the direction of the propagation. These waves are slower than P waves and their speed is defined by equation 2. The surface waves are the slowest. For its low frequency, long duration and large amplitude these can usually be the most destructive. There are several types of surface wave (such as Rayleigh and Love). For the Rayleigh (R) waves, which propagate along the surface, their velocity is approximately that defined in equation 3. These waves cause elliptical orbit displacements in the medium particles and their amplitude decreases rapidly with depth.

$$v_P = \sqrt{\frac{E(1-\nu)}{\rho(1+\nu)(1-2\nu)}} \tag{1}$$

$$v_S = \sqrt{\frac{E}{2\rho(1+\nu)}} \tag{2}$$

$$v_R = \frac{0.87+1.12\nu}{1+\nu}\sqrt{\frac{E}{2\rho(1+\nu)}} \tag{3}$$

3. Numerical model

The time-marching algorithm presented here is based on the finite element method and, applied to a dynamic, multidimensional and damped system, can be mathematically defined by equation 4,

$$\mathbf{F}(t) = \mathbf{F}_\mathrm{I}(t) + \mathbf{F}_\mathrm{D}(t) + \mathbf{F}_\mathrm{S}(t) \tag{4}$$

were $\mathbf{F}(t)$ is the applied load, $\mathbf{F}_\mathrm{I}(t) = \mathbf{M}\mathbf{U}(t)$ is the force of inertia, $\mathbf{F}_\mathrm{D}(t) = \mathbf{C}\mathbf{U}(t)$ is the damping force (considering a viscous damping) and $\mathbf{F}_\mathrm{S}(t) = \mathbf{K}\mathbf{U}(t)$ is the elastic force. $\mathbf{U}(t)$, $\mathbf{U}(t)$, $\mathbf{U}(t)$ are respectively the acceleration, velocity and displacement vectors dependent on time, t.
The governing equations of the algorithm and the time integration strategy are presented in [6], describing the basic aspects and the main parameters of this novel formulation using finite elements in the time domain. This paper presents only the time marching equations used in this new formulation, which are

$$\mathbf{E}\mathbf{U}^{n+1} = \mathbf{F}^{n+\frac{1}{2}} + \mathbf{M}\mathbf{U}^{n} \quad \frac{1}{2}\ t\mathbf{C}\mathbf{U}^{n} \quad \mathbf{K}\left(\ t\mathbf{U}^{n} + \frac{1}{2}\ t^{2}\mathbf{U}^{n}\right) \tag{5}$$

– the velocity equation – and

$$\mathbf{E}\mathbf{U}^{n+1} = \mathbf{E}\left(\mathbf{U}^{n} + \frac{1}{2}\ t\mathbf{U}^{n} + \frac{1}{2}\ t\mathbf{U}^{n+1}\right) \quad \frac{1}{2}\ t^{2}\mathbf{C}\mathbf{U}^{n+1} \quad \mathbf{K}\left((\beta b_1 b_2)\ t^{3}\mathbf{U}^{n} + \left(\frac{1}{16} + \beta b_1\right)\ t^{3}\mathbf{U}^{n+1}\right) \tag{6}$$

– the displacement equation – where $\mathbf{C}$ is the damping matrix, $\mathbf{E} = \mathbf{M} + \frac{1}{2}\ t\mathbf{C}$ is the effective matrix, $\mathbf{M}$ and $\mathbf{K}$ stand for the mass and stiffness matrices, respectively; $\mathbf{U}$, $\mathbf{U}$ and $\mathbf{F}$ stand for the displacement, velocity and load vectors,

respectively; n and t are the time-step number and time-step length, respectively; $\beta = 1, b_1 = 8.567 \times 10^{-3}$ and $b_2 = 8.590 \times 10^{-1}$ are the time integration parameters of the new method; $\overset{n+1/2}{\mathbf{F}} = \beta_1 \ t\mathbf{F}^n + \beta_2 \ t\mathbf{F}^{n+1}$, with $\beta_1 = \beta_2 = 1/2$, using trapezoidal quadrature rule or $\beta_1 = 1$ and $\beta_2 = 0$, extending the explicit feature of the technique to the load term (see [6] for more details). The main features of this model, among others, are: the method is based only on single-step displacement-velocity relations; it requires no system of equations to be dealt with; it is second-order accurate. In other words, this model is very effective, being able to provide accurate analyses considering relatively large time steps (thus, also being very efficient). Moreover, since it has high stability limits, it minimizes the main drawback of explicit procedures, allowing time-steps that are usual in accurate implicit analyses, rendering good results at reduced computational costs [6].

4. Numerical results

The strategy used in this article to evaluate the effect of the presence of inclusions on the vibrations registered in receivers, placed in the downstream zone, was to determine the inclusions insertion loss and then compare the results with classical devices, in this case, using buried walls with the same material characteristics of the inclusions.

To determine the inclusions' insertion loss, it was performed a study without any type of mitigating devices and then, a set of three parallelepiped inclusions with quadrangular base of 0.6 m width. Sets of inclusions with three distinct depths and two types of materials were studied. Finally, a wall with the inclusion width, at the distance of the closest inclusion of the load, with the same three depths and with the same material properties of the inclusions was considered. For all the studies a host medium with density ρ_m=1700 Kg/m^3, Young's modulus E_m=115.76×10^6 Pa and Poisson's ratio ν_m=0.33, was considered. These thirteen studies, summarized in the Table 1, where the mitigation devices material properties are defined, were performed using the finite element method that integrates the time-marching algorithm described above.

Table 1 – Summary of studies carried out

Study	mitigating devices				
	Type	Depth [m]	Density [Kg/m^3]	Poisson's ratio	Young's modulus [Pa]
M1	(no mitigating devices)				
I1	3 Inclusions	1	2100	0.25	2.7×10^9
I2		3			
I3		5			
I4		1	2700	0.2	27×10^9
I5		3			
I6		5			
W1	Wall	1	2100	0.25	2.7×10^9
W2		3			
W3		5			
W4		1	2700	0.2	27×10^9
W5		3			
W6		5			

The geometric scheme of the model is shown in Figure 2. In this figure, an absorption layer is shown, 6 m wide, necessary to define an infinite medium in the model. This layer, which has the width of at least one wavelength, is responsible for absorbing all the energy that enters it, avoiding unwanted reflections in the system under study. Since the propagation domain is infinite, the load is a line load, and the structure is repeated infinitely along one direction, only a 1.2 m wide slice was modeled, and adequate boundary conditions were used to simulate the infinite character of the problem. The system is excited by a Ricker pulse whose source is located 10 m right of the system origin. The mitigation devices begin 10 m to the right of the excitation point. The proposed mitigation device consists of a periodic set of three inclusions spaced apart by 0.6 m. Three sets of inclusions are considered, with different depths of 1, 3 and 5 m. In addition, two different materials were considered for the inclusion (see Table 1). To demonstrate the efficiency of these devices, the effect of a buried wall, 10 m from the source of excitation, was also studied. Similar to the three sets of inclusions, three wall depths were considered, and with the same materials used in the inclusions.

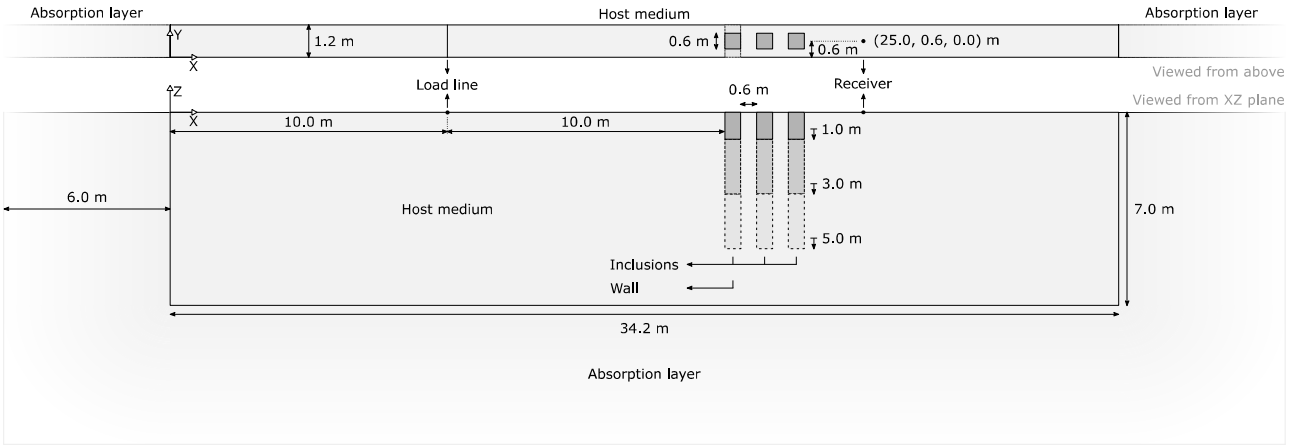

Figure 2– Schematic representation of the model used for the wave propagation analysis

Numerical simulations were performed using the 3D finite element method in the time domain, formulated using regular tetrahedral elements. The time marching algorithm described above was recently developed by Soares Jr. [6] and is adopted to render the numerical process more efficient. A damping factor equal to 1% and a propagating Ricker pulse with a central frequency of 60 Hz were considered.

Figure 3 shows the results obtained with a set of three lines of inclusions and with a buried wall, both with 5 m depth, comparing the response for the propagation in a homogeneous medium with that considering the different devices, with a) a poorer material and b) a stiffer material. Note that the difference in stiffness in the buried wall material does not lead to a significant difference in results. Of the studied cases, this difference is more pronounced in the 3 m depth wall (not shown). Another note that can be made by observing this figure is that the set of poorer inclusions produces practically the same result as the buried stiff wall.

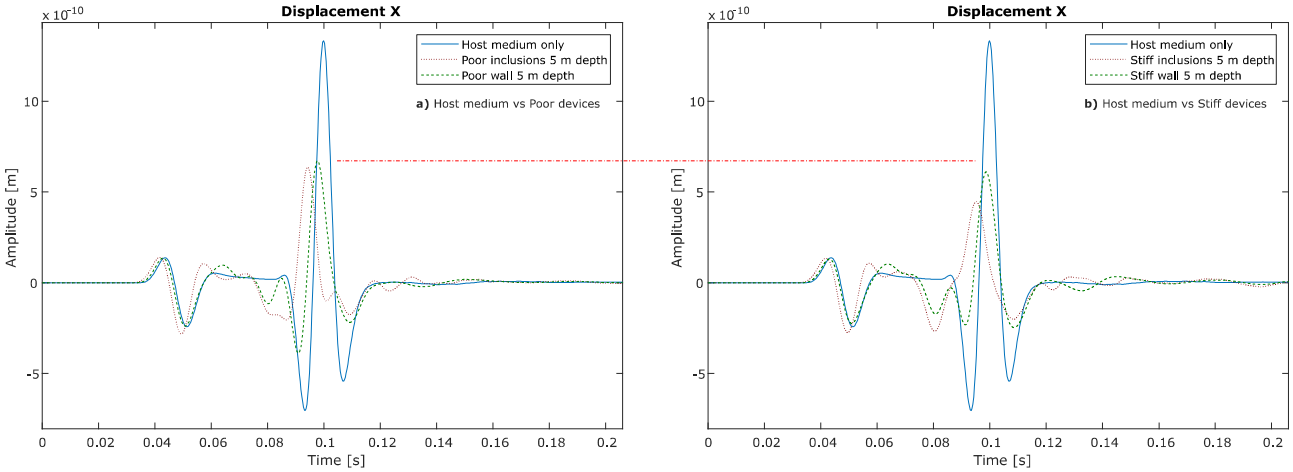

Figure 3– Comparison between types of mitigation devices, 5 m depth, and their stiffness: a) poor and b) stiff

Figure 4 shows snapshots of the wavefield, in terms of horizontal displacements, computed in the presence of a set of inclusions and of a buried wall. Here, the interference of the buried devices is clear, with a more complex wave pattern being visible when multiple inclusions are considered. This is particularly evident for later times. These snapshots also evidence that a considerable fraction of the energy is reflected back by both the inclusions and the wall, showing the intended shielding effect. Additionally, from these figures surface waves seem to have a strong importance, as expected. It can also be seen that no spurious reflections from the artificial damping layer seem to occur.

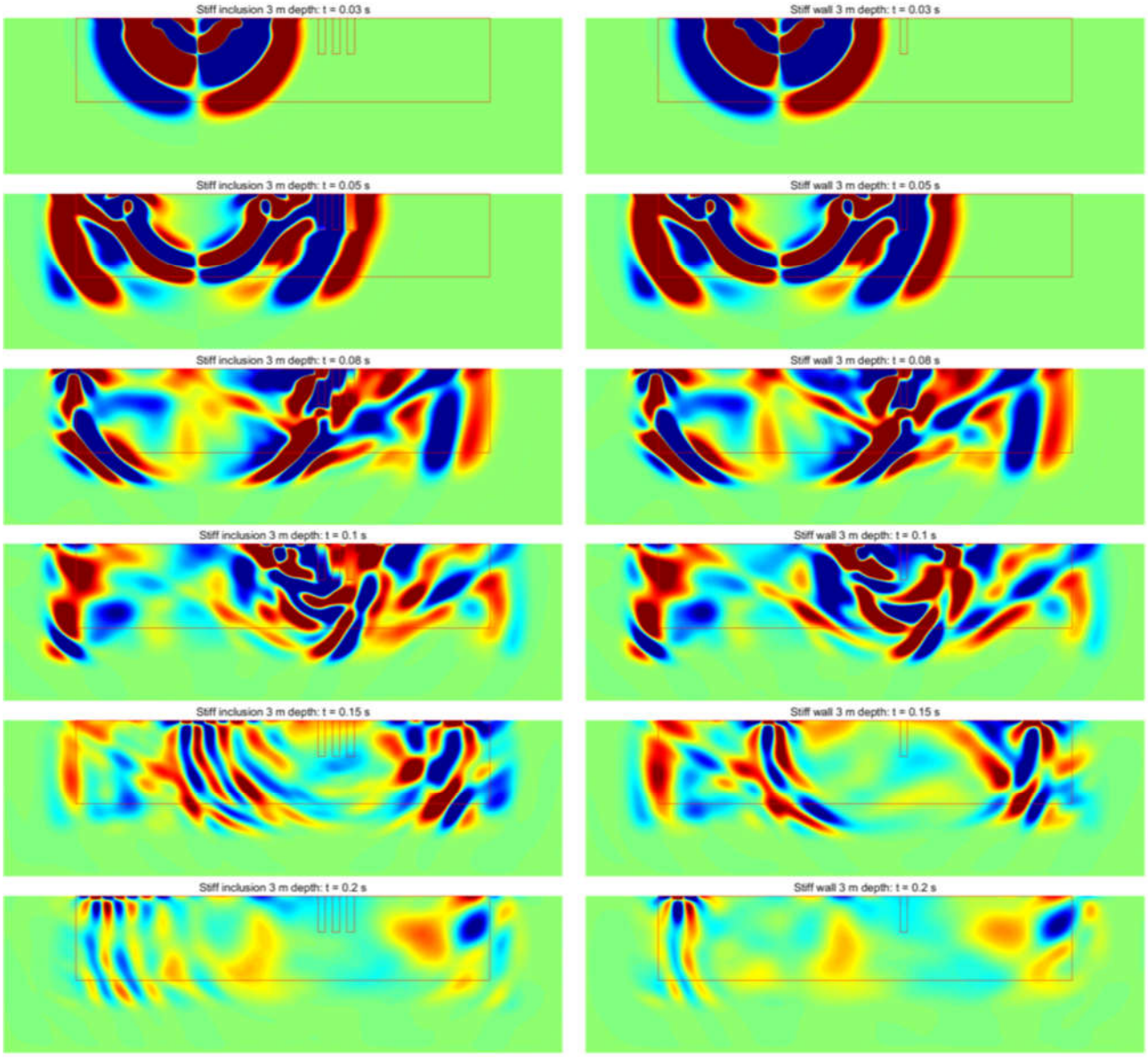

Figure 4– Temporal evolution: stiff inclusions 3 m depth (left) and stiff wall 3 m depth (right)

Figures 5 and 6 show the vibration levels detected at a receiver 25 m from the source, beyond the mitigation devices. These levels are computed in the frequency domain, after application of a Fourier-transform to the time signals computed using the TD-FEM algorithm. To better observe the global behavior, the response is grouped in frequency bands 16 Hz wide.

From these figures, it can be seen that all sets of mitigation measures allow a reduction of the vibration levels, although acting differently throughout the frequency range.

To better understand the results, Figure 7 shows the reduction of vibration estimated for each scenario, for the three depths studied, and for the two types of elastic material composing the inclusions and walls. To evaluate the effect of the presence of mitigation devices in the vibrations registered in the receiver, the reduction is computed in terms of insertion loss, IL, that is defined as the difference between the vibration levels obtained in the presence of mitigation devices ($L1$) and the displacement vibration levels obtained without those devices ($L0$). This is given in dB by the following Equation 7:

$$IL = L0 \quad L1 = 20\log|u_0| \quad 20\log|u_1| \quad (7)$$

According to Equation 7, positive values correspond to a reduction of the displacement vibration levels in the presence of mitigation devices and negative values of the insertion loss stand for losing protective solutions efficiency.

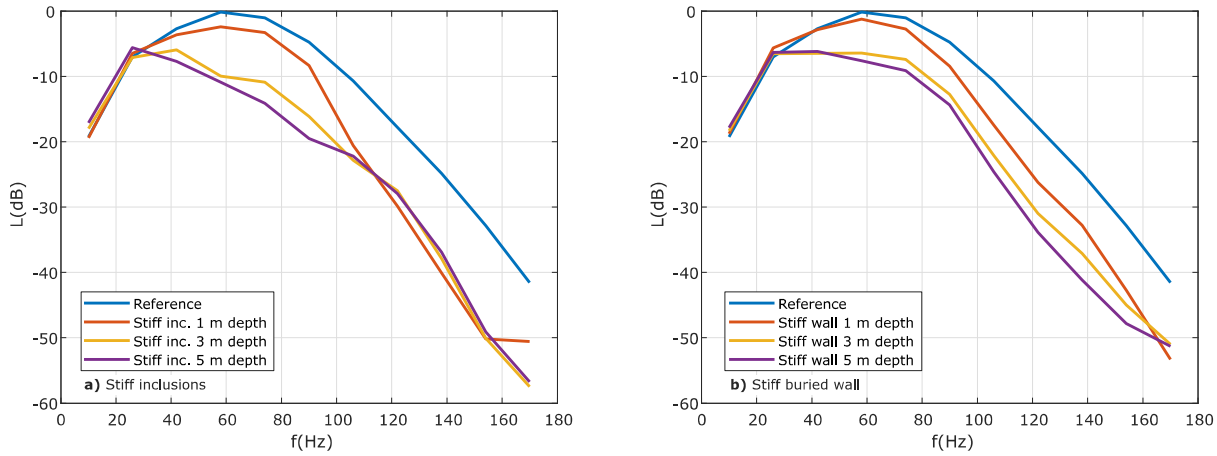

Figure 5– Vibration levels with a) stiff inclusions and b) buried walls

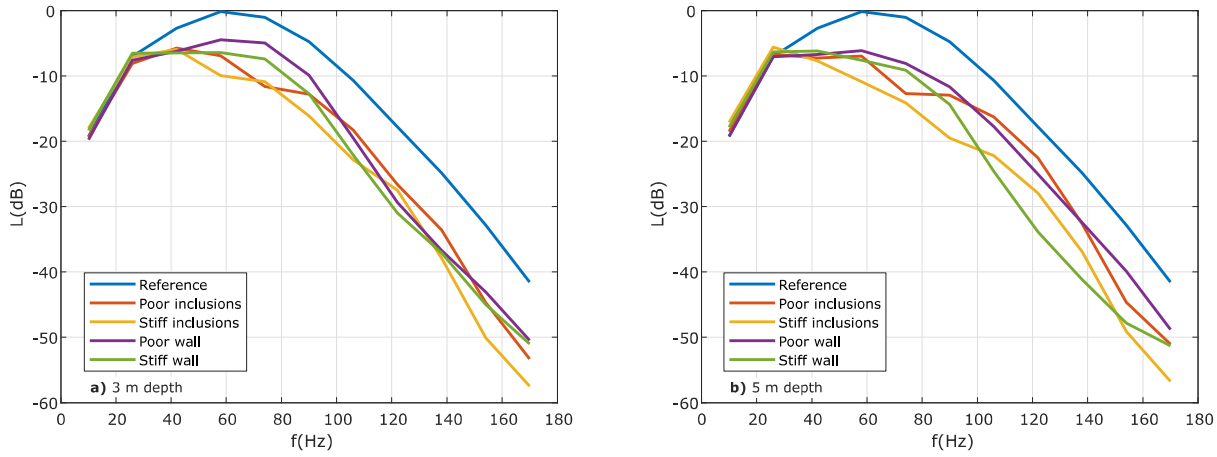

Figure 6– Vibration levels with a) 3 m and b) 5 m depth of mitigation devices

From the results in Figure 7 it becomes clear that the insertion loss tends to increase with the frequency of the excitation load. However, it seems that for the case of the periodic array of inclusions a peak in the insertion loss occurs between 40 and 100 Hz, for which frequencies the efficiency of this solution surpasses that of the traditional buried wall. If surface (Rayleigh) waves are considered, which propagate in the soil with an approximate velocity of 149 m/s, and taking into account that the inclusions are equally spaced 1.2m, this frequency range seems to match what is usually considered as the band gap frequency in sonic crystals (f=c/2d), which should occur around 62Hz. This finding is quite important, and indicates that the mitigation solution can be tuned depending on the frequency band to mitigate and on the properties of the host medium. It should be noted that this effect is even more pronounced when inclusions (and walls) 5m deep are considered, as depicted in Figure 7b. For this case, a peak is quite evident in the identified frequency interval, for which IL values around 4dB higher than those computed for the buried walls of the same material are registered. It should also be said that the more traditional solution of a buried wall seems to reach improved performance for higher frequencies, and to have a broader frequency range for which vibration attenuation is provided.

Regarding the type of material used in the protection devices, it can be seen that, as expected, using a stiffer material leads to a better performance, with higher values of insertion loss being reached. Indeed, for this case a stronger contrast of properties between the soil and the devices exists, and allows stronger energy reflections to occur.

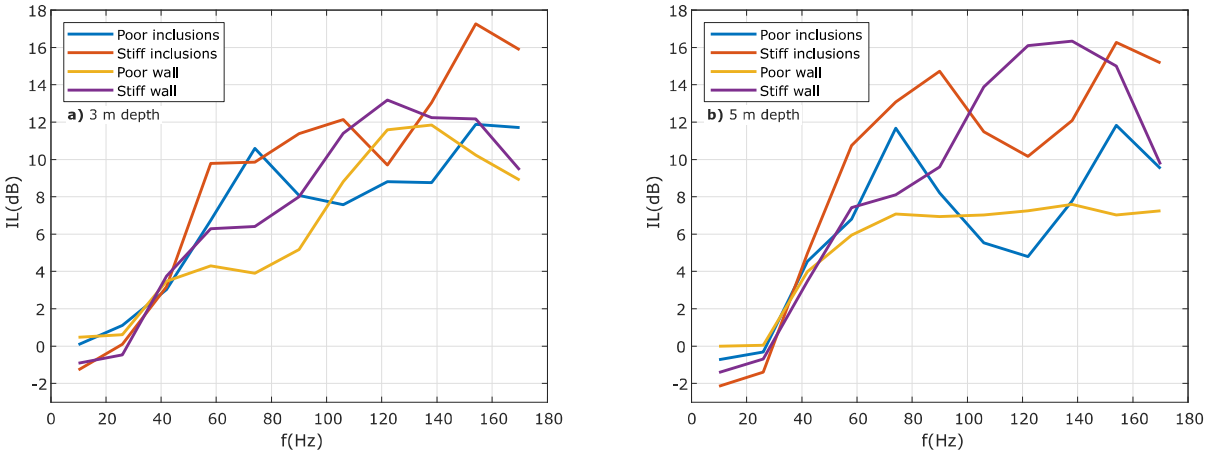

Figure 7– Insertion loss of the mitigation devices with depths of a) 3 m and b) 5 m.

5. Conclusions

This paper has presented and studied the effect of a periodic set of buried inclusions in the propagation of vibrations in a homogeneous soil. A TD-FEM algorithm is used for that purpose, making use of a recently proposed and efficient time marching scheme. The computed results are quite promising, and reveal the existence of a specific frequency band for which higher vibration attenuation seems to occur. These band can be related to the effect of multiple interactions between the buried inclusions, as is usually seen in acoustics when analyzing sonic crystals.

Acknowledgement

The authors acknowledge the financial support of FCT – Foundation for Science and Technology and COMPETE, through research project PTDC/ECM-COM/1364/2014 (METASHIELD). This work is also financed by FEDER funds through the Competitivity Factors Operational Programme - COMPETE and by national funds through FCT – Foundation for Science and Technology within the scope of the projects POCI-01-0145-FEDER-007633 (ISISE) and POCI-01-0145-FEDER-007457 (CONSTRUCT). The authors acknowledge the financial support of Regional Operational Programme CENTRO2020 within the scope of the project CENTRO-01-0145-FEDER-000006 (SUSpENsE).

References

[1] Y. B. Yang; H. H. Hung, Wave Propagation for Train-Induced Vibrations. A Finite/Infinite Element Approach, Singapore, World Scientific Publishing Co Pte Ltd, 2009.

[2] P. Amado Mendes, L. Godinho: Reduction of Vibrations Transmitted Through the Soil by Multiple Buried Inclusions – Numerical Analysis. Proc. 11th International Conference on Vibration Problems, Lisbon, Portugal, 2013.

[3] C. Albino, L. Godinho, D. Dias-da-Costa, P. Amado-Mendes: The MFS as a tool for the numerical analysis of vibration protection devices, Proc. ICA2016, Buenos Aires, Argentina, 2016

[4] A. Castanheira-Pinto, P. Alves-Costa, L. Godinho, P. Amado-Mendes: Mitigation of vibrations induced by railway traffic though soil burried inclusions: a numerical study. Proc. Tecniacústica 2017, A Coruña, Spain, 2017.

[5] L. Godinho, P. Amado-Mendes, P. Alves-Costa, C. Albino: MFS Analysis of the Vibration Filtering Effect of Periodic Structures in Elastic Media. International Journal of Computational Methods and Experimental Measurements, Vol.6, Issue 6 (2018), 1108-1119.

[6] D. Soares Jr.: A novel family of explicit time marching techniques for structural dynamics and wave propagation models, Computer Methods in Applied Mechanics and Engineering, 311 (2016), 838-855.